


4,8-dicarboxyl-8,9-iridoid-1-glycoside Promotes Neural Stem Cell Differentiation Through MeCP2

Dose-Response:
An International Journal
July-September 2022:1–10
© The Author(s) 2022
Article reuse guidelines:
sagepub.com/journals-permissions
DOI: [10.1177/15593258221112959](https://doi.org/10.1177/15593258221112959)
journals.sagepub.com/home/dos


WeiBing Wang^{1,*} , Zhen Liu^{2,*}, BaoSheng Jing² , HaiMin Mai³, Hong Jiao⁴, Teng Guan^{5,*}, DanGui Chen⁶, JiMing Kong^{5,*}, and Tao Pan^{2,*}

Abstract

Background: Borojó (Borojoa patinoi Cuatrec) fruit has recently been shown to have a variety of health benefit, but the mechanisms have been little studied. The aim of this study was to investigate the effect of 4,8-dicarboxyl-8,9-iridoid-1-glycoside (388) on proliferation and differentiation of embryonic neural stem cells (NSCs).

Methods: NSCs were treated with 388 and stem cell differentiation was determined by western blotting and immunofluorescence staining. The role of MeCP2 in 388-mediated embryonic NSCs differentiation was examined.

Results: The results showed that in the presence of mitogen when NSCs proliferated and maintained their multipotency, treatment with 388 did not affect the viability of NSCs. Following mitogen withdrawal to initiate NSC differentiation, treatment with 388 at the doses of 10 and 50 µg/mL significantly increased neural differentiation in both cortex and spinal cord-derived culture. 388 also significantly up-regulated MeCP2 expression. The expression of the neuronal and oligodendrocytic markers was enhanced after addition of 388 in the differentiation culture. However, knockdown of MeCP2 results in inhibition of NSC differentiation, and the pro-differentiation effect of 388 was mostly abolished.

Conclusions: This study confirmed that 388 stimulates differentiation of NSCs and identifies its mechanism of action by upregulating MeCP2.

Keywords

Borojó, 4,8-dicarboxyl-8,9-iridoid-1-glycoside, embryonic neural stem cells, MeCP2

¹ Department of Anesthesiology, The Affiliated AnQing Municipal Hospitals of Anhui Medical University, AnQing, China

² Department of Orthopedic, The Affiliated AnQing Municipal Hospitals of Anhui Medical University, AnQing, China

³ Department of Human Anatomy and Cell Science, The Sixth Affiliated Hospital of Sun Yat-sen University, GuangZhou, China

⁴ Guangzhou Bolojo Biological Technology Co. Ltd., GuangZhou, China

⁵ University of Manitoba, Winnipeg, MB, Canada

⁶ Department of Hematology, The affiliated AnQing municipal hospitals of Anhui Medical University, AnQing, China

Received 14 May 2022; received revised 15 July 2022; accepted 23 July 2022

*These authors have contributed equally to this work.

Corresponding Authors:

Jiming Kong, Department of Human Anatomy and Cell Science, University of Manitoba, 745th Bannatyne Avenue, Winnipeg, MB R3E 0J9, Canada.
Email: jiming.kong@umanitoba.ca

Tao Pan, The Affiliated AnQing Municipal Hospitals of Anhui Medical University, 87th Tianzhushan East Road, AnQing 246003, China.
Email: pantao@126.com



Creative Commons Non Commercial CC BY-NC: This article is distributed under the terms of the Creative Commons Attribution-NonCommercial 4.0 License (<https://creativecommons.org/licenses/by-nc/4.0/>) which permits non-commercial use, reproduction and distribution of the work without further permission provided the original work is attributed as specified on the SAGE and

Open Access pages (<https://us.sagepub.com/en-us/nam/open-access-at-sage>).

Introduction

Iridoid is a class of compounds and the main compositions of natural products across several plant families, including the Apocynaceae, Lamiaceae, Loganiaceae, Rubiaceae, Scrophulariaceae, and Verbenaceae.¹ Iridoids are cyclopentanoid monoterpene derivatives, most frequently occur in plants combined with sugar and so are classified as glycosides. Iridoid glycosides offer a broad range of biological effects, such as antidiabetic, anticancer, anti-inflammatory and neuroprotective potency. The iridoid boschnaloside isolated from *Boschniakia rossica* is shown to improve diabetic symptoms including fasting blood sugar, hemoglobin A1c, glucose in tolerance, and Homeostatic Model Assessment of insulin resistance through modulating the action of glucagon-like peptide-1.² Iridoid glycosides Kutkin, Kutkoside, and Picroside I, from *Picrorrhiza kurroa*, directly interact and dose-dependently inhibit MMP-9 activity and are proposed to be developed as anticancer agents.³ In addition, cornel iridoid glycoside significantly ameliorates neuroinflammation by inhibiting apoptosis in rats with brain injury.^{4,5} Most notably, it is suggested that iridoid glycoside promotes neurogenesis and improve axonal regeneration by boosting neuronal differentiation and neurite outgrowth in neural stem cells.^{6,7} Therefore, in recent years, there is increased interest in the research on iridoid glycosides.

Borojó (*Borojoa patinoi* Cuatrec) fruit belongs to the Rubiaceae family and is a principal source of iridoid glycosides, Borojó fruit is also shown to possess high antioxidant activity which may underlie its beneficial health effect and pharmacological potential.⁸ Borojó fruit is predominantly found in the tropical rainforest of the Colombian Pacific region with reported antihypertensive, antitumoral, diuretic, healing, immunological, anti-inflammatory, and aphrodisiac effects, and previous phytochemical studies reveal that the Borojó aqueous extract exhibits antimicrobial activity against the *P. aeruginosa*.⁹

Nutritional values and therapeutic applications of some types of iridoid have been reported in many studies, and one type of iridoid glycoside has been shown to modulate Methyl CpG binding protein 2 (MeCP2), a transcriptional repressor.¹⁰ The effect of an iridoid glycoside on MeCP2 has important implications in stem cell biology. MeCP2 is a multi-function factor involved in locus-specific transcriptional modulation and the regulation of genome architecture. The MeCP2 gene is ubiquitously expressed, and its mutations are associated with Rett syndrome. Mutations in MeCP2 impair the function of many genes in neural stem cells, as well as in other tissues and organs. Specifically, MeCP2 alters the stem cell activity, which in turn, profoundly affects the life of an individual. Reduced expression and activity of MeCP2 in neural stem cells are connected with senescence, proliferation impairment, and unrepaired DNA foci accumulation.¹¹ In neurons lacking MeCP2, the endogenous galactosidase activity shows a significant increase in P53 activity and senescence.¹² Whether the beneficial health effect of Borojo fruit can be attributed an effect on MeCP2 of its active component has never been explored. We

have recently performed systematic chemical structure analysis and identified the active component of Borojo fruit as 4,8-dicarboxyl-8,9-iridoid-1-glycoside (388).^{13,14} This chemical exhibits strong antioxidant activity.¹⁵ An immediate question is to ask if 388 could exert an effect on MeCP2 function. The answer to this question may explain the functional properties of Borojó fruit and facilitate nutritional and pharmacological application of this natural fruit in neuroprotection and neural regeneration through stem cell regulation.

This study aimed to test the hypothesis that of the Borojó main active component 388 promotes neuronal cell differentiation via action on MeCP2 activation. We therefore compared the neural differentiation process in neural stem cells that treated with 388 extracted from Borojó. We also analyzed the effect of 388 on MeCP2 and neural differentiation in MeCP2 silenced stem cells. With both cortex and spinal cord-derived models, we have demonstrated that the 388 stimulates neural cell differentiation, at least in part due to activation of MeCP2.

Materials and Methods

Chemicals and Animals

Dulbecco's modified Eagle Medium (DMEM), neural basal medium, B27 supplement, KnockOut™ DMEM/F-12 medium, StemPro™ Neural Supplement, StemPro Accutase, FGF-basic (AA 10–155) recombinant human Protein, EGF Recombinant Human Protein were purchased from ThermoFisher Canada. Modified ITS culture supplement was purchased from Wisent Canada., Poly-D-lysine and laminin were obtained from Sigma-Aldrich (St. Louis, MO, USA). The antibodies used were as follows: Antibodies: Anti-MAP2 antibody: Abcam Cat# ab28032; Anti-MeCP2 antibody: Abcam Cat# ab2828; Anti-PDGFR-alpha: Abcam Cat# ab96569; Anti-Myelin Basic Protein antibody: Abcam Cat# ab218011; Anti-GFAP Antibody: ThermoFisher Scientific Cat# PA1-10004; Anti-Neurofilament H (NF-H), Phosphorylated antibody: BioLegend Cat# 801602; Anti-beta-actin antibody: Novus Cat# NB100-56874; Anti-beta 3 Tubulin antibody: Santa Cruz Biotechnology Cat# sc-80005. Timed pregnant Sprague–Dawley rats were obtained from Central Animal Care Services at the University of Manitoba. Animals were housed under temperature-controlled conditions with a 12 hours light/dark cycle and ad libitum access to water and food. All efforts were made to minimize animal suffering and reduce the number of animals used.

Plant Material Collection, Extraction and Isolation 388 Preparation

Borojó pulp was heated at 70°C for extraction, and the semi-prepared ultraviolet 254 nm absorption peak fractionation was used to extract the main active substance 388 of Borojó. By analyzing and inferring the structure of the active extract through nuclear magnetic resonance and infrared spectroscopy, (Figures 1 and 2), it can be determined that: The

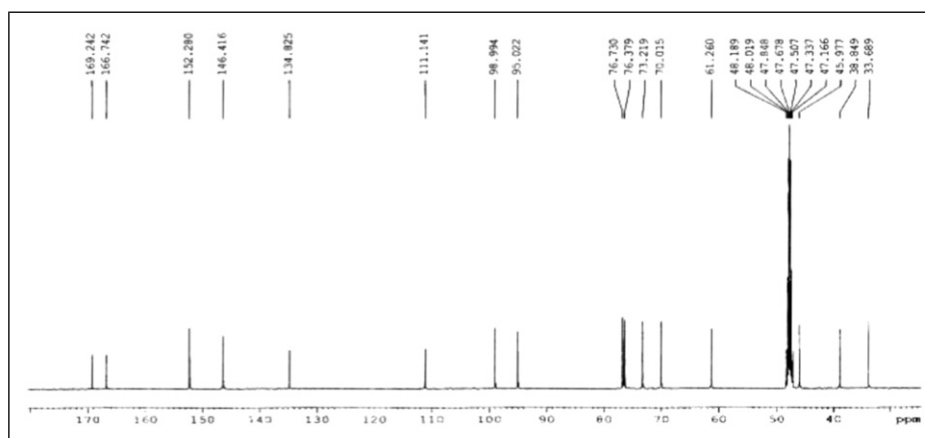


Figure 1. Actual NMR carbon spectrum of Borojó active substance.

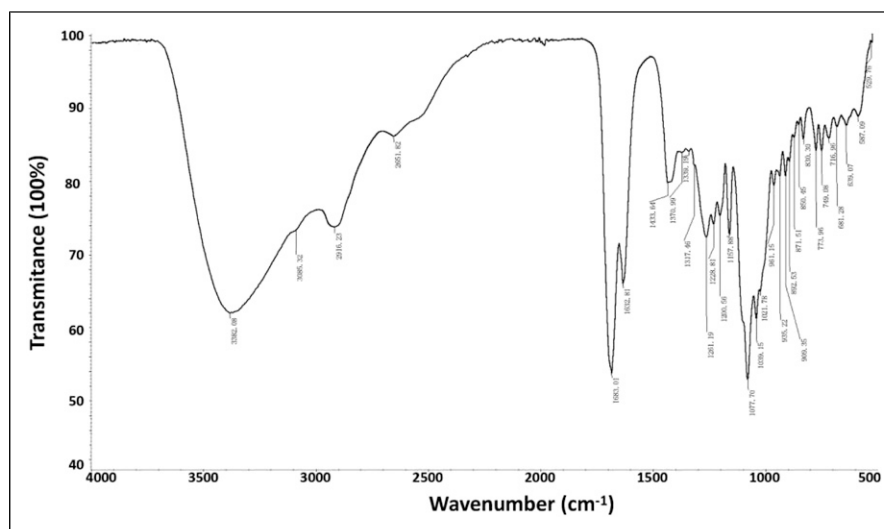


Figure 2. Infrared spectrum of Borojó active substance.

molecular structure of Borojó's main active substance (substance with mass number 388) is: Chemical name: 4,8-dicarboxyl-8,9-iridoid-1-glycoside. Molecular formula: $C_{16}H_{20}O_{11}$. Exact molecular weight: M/Z 387.09289. Chemical Structure: (Figure 8)

Cortex and Spinal Cord-Derived Stem Cell Culture

Timed pregnant Sprague–Dawley rats were humanely euthanized by CO_2 gas followed by cervical dislocation, and embryos were removed. Cortex-derived stem cell culture was prepared as described previously (Theresa K. Kelly et al 2009). The day of the positive vaginal plug was considered as E0.5 of pregnancy and embryos were collected at E14.5 and placed in Hanks' Balanced Salt Solution (HBSS, without Ca^{2+} and Mg^{2+}) solution on ice. The brain was removed and after removing the meninges and other connective tissue, the entire cerebral cortex from both hemispheres was dissected out, triturated, and cells passed through a $40\ \mu m$ mesh. Cells were maintained in complete StemPro NSC media containing

FGF-basic (AA 10–155) Recombinant Human Protein (bFGF) (20 ng/mL) and EGF Recombinant Human Protein (hEGF) (20 ng/mL), in order to maintain NSC characteristics. After neurosphere expansion for 1 week, the NSCs were dissociated for NSC differentiation studies. The NSCs were harvested by centrifugation and plated on a PDL and laminin coated plates in complete StemPro NSC medium. Then, the medium was changed to a neural differentiation medium (neurobasal/B27) after 2 days of culture. The cells were fed every third day by aspirating half of the medium from each well and replacing it with fresh neural differentiation medium.

The procedures for rat E16 spinal cord-derived culture were similar to those described from the cortex as described (Thomson et al 2008). Briefly, spinal cords from embryos were collected in a petri dish containing HBSS (without Ca^{2+} and Mg^{2+}). After carefully removing the meninges, the spinal cord tissue was cut into small pieces with a surgical blade. The minced tissue was then transferred into a 15-mL centrifuge tube with 1 mL StemPro Accutase and incubated for

20 minutes at 37°C for enzymatic dissociation. The dissociated cell suspension was then passed through a 40 µm cell strainer. Cells were then seeded on poly-L-lysine-coated coverslips at a density of $4 \times 10^5/\text{cm}^2$. After 2 hours adhesion, the plating medium (50% DMEM, 25% HBSS, and 25% horse serum) was replaced with differentiation medium (DMEM and modified ITS culture supplement). At DIV14, insulin was excluded from the culture system.

WST-1 Cell Proliferation Assay

For the WST-1 cell proliferation assay, a total of approximately $.25 \times 10^5$ cells were cultured in each well of a 96-well plate in a final volume of 100 µL. Triplicates of each condition were prepared. These cells were exposed to either vehicle (DMSO) or 388 at different concentration for 48 hours. After the treatment, WST-1 proliferation reagent (#ab 155902, Abcam, Cambridge, UK) was added to each well, and the assay was performed in accordance with the manufacturer's instructions. Experiments were performed in triplicate in three independent experiments.

NSCs Transfection, and RNAi

The NSCs were placed in a 24-well plate with $1.0 \times 10^5/\text{mL}$, and 0.5 mL/well. NSCs were culture at 37°C in 5% CO₂ for 24 hours. To prepare the first tube of reagent: add 3 µL Lip3000 solution to 75 µL OPTI-MEM. Second tube reagents: 4.2 µL (2.1 µg) shRNA plasmid was added to 75 µL OPTI-MEM, 3 µL P3000 was added and mixed. Mix the first tube of reagent and the second tube of reagent according to 1:1 at room temperature for 15 minute. Add 50 µL/well into the corresponding petri dish and continue culture at 37°C in 5% CO₂. The transfection efficiency was observed under fluorescence microscope 24 hours later. The expression level of MeCP2 was detected by qPCR, a knockdown effect greater than 70% is considered effective.

Western Blotting

The total cellular samples were washed two times with ice-cold PBS, scraped with IP lysis buffer, and then transferred into a micro centrifuge tube. The cell suspension was maintained with constant agitation for 30 minutes at 4°C. Then the cell lysate was centrifuged at $21\,000 \times g$ for 30 minutes at 4°C and supernatants were collected for analysis. The protein concentration was determined using BCA Protein Assay Reagent (Pierce, Rockford, IL, USA).

Samples were boiled for 5 minutes in Laemmli sample buffer containing 2.5% β-mercaptoethanol and 10 µg of sample proteins were separated by 12% TGX Stain-Free polyacrylamide gels (Cat#1610185, Bio-Rad), and transferred to PVDF membrane by Trans-Blot Turbo Transfer System (Bio-Rad). Membranes were blocked with 5% (w/v) fat-free dry milk in Tris-buffered saline (10 mM Tris-HCl, pH

7.5, 150 mM NaCl) containing .05% Tween-20 for 1 hour and incubated with primary antibodies overnight at 4°C. Blots were washed 3 times in TBS buffer and then incubated with appropriate secondary antibodies for 1 hour at room temperature. The protein bands were visualized with the enhanced chemiluminescence reagent (ECL Prime, GE Healthcare, Cat# RPN2232) by an imager (ChemiDoc MP, imaging system, Bio-Rad).

Immunocytochemistry

Cells were grown on coverslips coated with PDL. Cells were fixed in 4% paraformaldehyde in PBS pH 7.4 for 15 minutes at room temperature and then were washed 3 times with PBS. Samples were incubated for 10 minutes in PBS containing .25% Triton X-100 (PBST) to improve penetration of the antibody. After 3 times of wash with PBS, coverslips were incubated in 1% BSA in PBST for 30 minutes to block nonspecific binding of the antibodies. After blocking, samples were incubated with Ki-67, MAP2, and MeCP2 antibodies in 1% BSA overnight at 4°C. Following with three additional washes, secondary antibodies were applied and incubated for 1 hour at room temperature in the dark. After being washed three times, cells were incubated with Hoechst 33342 (Calbiochem) to counterstain for nuclei, and then coverslips were mounted with a drop of fluorescence mounting medium (Dako North America, Inc. Carpinteria, CA 93013, USA). These slides can be stored in the dark at -20°C or +4°C. Fluorescence pictures were taken on a Carl Zeiss Axio Imager Z2 microscope and processed with Zen Pro imaging software (Zeiss, Germany). For Ki-67 staining, the number of positive cells in five random fields was counted using Image J.

Statistical Analysis

SPSS17.0 version (SPSS Inc., Chicago, IL, USA) was used for all statistical analyses. Parametric data expressed as mean ± standard deviation (mean±SD), One-way analysis of variance (one-way ANOVA) was used for comparisons between groups. Kruskal-Wallis test was conducted for analysis of normalized data. A *P*-value less than .05 was considered statistically significant.

Results

388 Has No Effect On NSC Cell Viability, However, Suppresses its Proliferation

After neurosphere expansion for 1 week, the NSCs were dissociated and 1.0×10^4 cells were plated onto PDL/laminin-coated 96-well plates (Corning, NY, USA) for 24 hours followed by DMSO or 388 treatment for 24 hours. WST-1 cell assay was used to assess the effect of 388 treatment on the cell viability of embryonic neuron stem cells (NSC) derived from embryonic cortex. This proliferation assay was conducted in

the presence of bFGF and EGF. Results show that there was no significant difference of the cell viability among each group relative to the control group after incubation with 388 at a concentration range from 7.8 ~ 500 $\mu\text{g}/\text{mL}$ (Figure 3A). Moreover, after 24 hour of 388 incubation, a marked decrease of Ki-67 expression were noted after 10 $\mu\text{g}/\text{mL}$ 388 incubation relative to control, albeit no significant difference. This dose-dependent reduction in Ki-67 expression became apparent after exposure to 50 $\mu\text{g}/\text{mL}$ 388 as well as at the concentration of 100 $\mu\text{g}/\text{mL}$ relative to that of control even with presence of the mitogen ($*P < .05$; $***P < .001$, respectively) (Figure 3B).

Treatment of 388 Induces Neuronal and Oligodendrocytic Differentiation

Of the tested compounds, 388 showed a neurogenic effect (Figure 4A). The effect of 388 on the expression of neuronal marker was examined in cortex and spinal cord-derived cultures.

Spontaneous differentiation of NSC was induced by withdrawing bFGF and EGF from the culture medium and replacing differentiation medium. 388 was then added to the

cultures at different concentration, that is, 24 hours after plating for the cortex-derived culture and 2 weeks after plating after spinal cord-derived culture, respectively. The medium was changed every three days, while the 388 was also supplemented. After 7 days, cell cultures were collected for neuronal marker analysis. A marked dose-dependent increase of expression of dendritic marker protein MAP2 was noted in 388-treated cells. The effect became statistically significant after exposure of cells to 50 and 100 $\mu\text{g}/\text{mL}$ 388 (Figure 4A). Consistent with these results, co-immunofluorescence staining of MAP2 and MeCP2 revealed that the cell number of MAP-2 positive cells significantly increased in the presence of 388 when compared to that of the control group and majority of the MAP2 expressing cells were also MeCP2 positive (Figure 4C). The similar effect was also observed in the spinal cord-derived culture; 50 $\mu\text{g}/\text{mL}$ of 388 significantly increased the expression of PNFH protein, a neuronal cytoskeleton protein in spinal cord-derived culture. Interestingly, exposure of cells to 100 $\mu\text{g}/\text{mL}$ 388 did not discernibly alter the expression of PNFH protein (Figure 4B).

Since both cortex and spinal cord culture were derived from embryonic rat CNS tissue, we sought to identify the

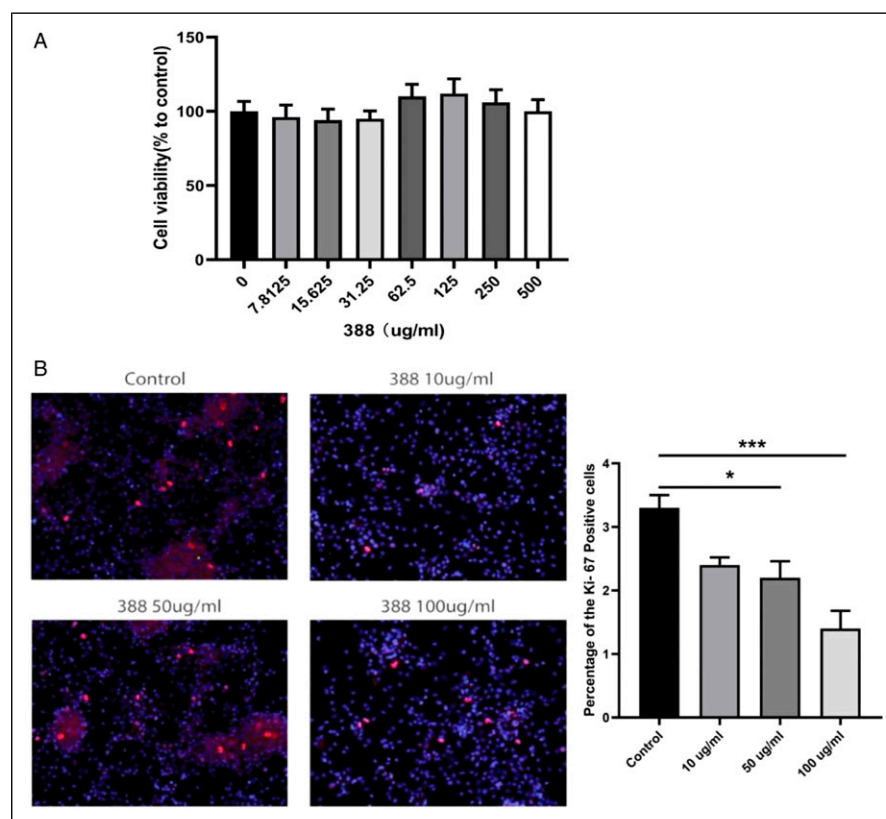


Figure 3. 388 compound has no effect on NSC cell viability; however, it could induce decline of cell proliferation. (A) The WST-1 measurement showed that there was no significant difference among the groups with 388 treatments at various concentrations. (B) Representative pictures of immunofluorescent staining for Ki-67 expression (magnification 200 \times). N = 5, $*P < .05$; $***P < .001$ verse control. NSC cells were incubated with 388 for 24 hours. The experiment was performed in triplicate. Results shown represent mean \pm SD from 3 independent experiments.

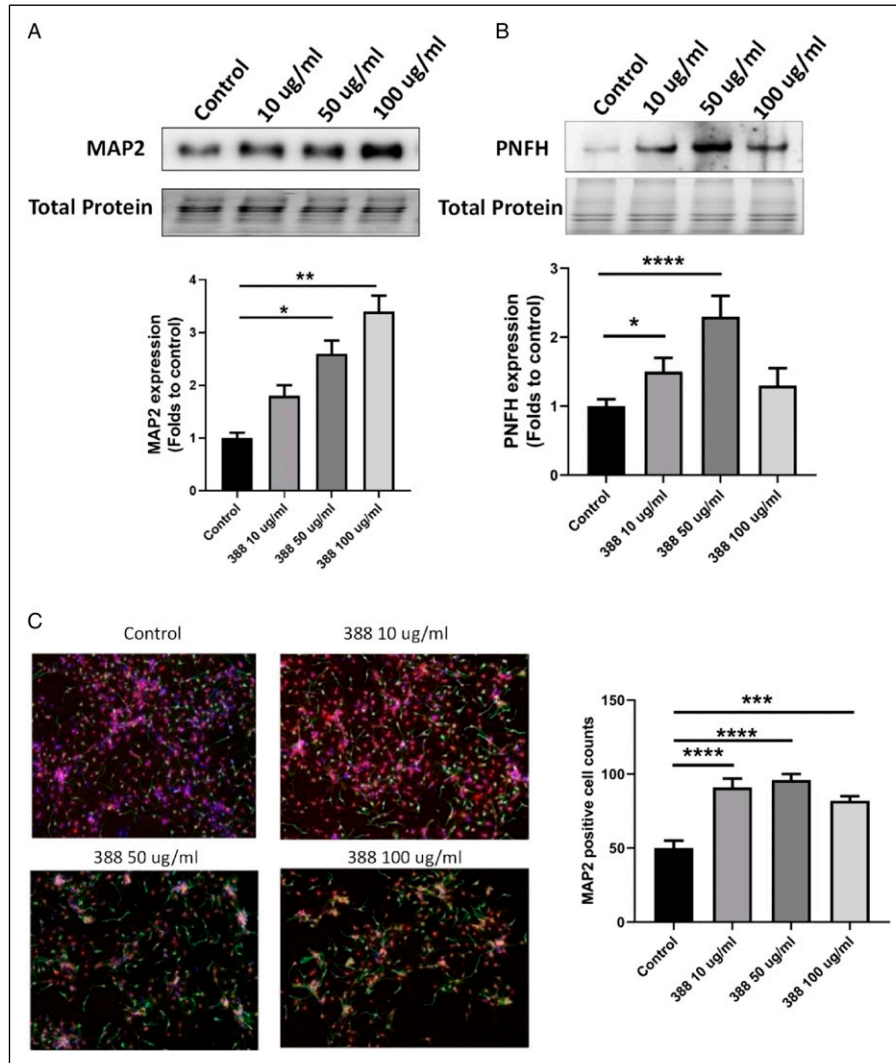


Figure 4. Treatment of 388 results in upregulation of MAP2 and PNFH expression in NSC. (A) MAP2 expression from NSC treated with 10, 50 and 100 $\mu\text{g}/\text{mL}$ 388 for 7 days of spontaneous differentiation. WT cortical neuron pretreatment with 388 for 24 hours, then OGD treatment for 1 hour, recovery for 24 hours. (B) PNFH expression from NSC treated with 10, 50, and 100 $\mu\text{g}/\text{mL}$ 388 for 7 days of spontaneous differentiation. Equal volumes of lysates with a total of 10 μg protein was applied to 12% TGX stain-free polyacrylamide gels. Total protein generated by stain-free visualization were used to ensure equivalent loading. Spontaneous differentiation was induced by withdrawing bFGF and EGF from the culture medium. 388 was added to the culture at different concentration. The medium was changed every 3 days, while the 388 was also added again. After 7 days, cell cultures were collected for PNFH expression analysis. (C) Co-immunofluorescence staining of MAP2 and MeCP2 after treatment with 388. One-way ANOVA followed by Bonferroni's Multiple Comparison Post-Test were performed to establish significant differences with control group: * $P < .05$; *** $P < .01$; **** $P < .001$. The experiment was performed in triplicate. Results shown represent mean \pm SD from 3 independent experiments.

differential effect of 388 on spinal cord-derived culture. Similar to MAP2 expression of cortex-derived culture, platelet-derived growth factor (PDGF)- α expression increased significantly in all three doses of 388 (Figure 5A). However, only 10 $\mu\text{g}/\text{mL}$ 388 resulted in an increase in the expression of MBP, a main constituent of myelin sheath, compared with that in control, while 50 $\mu\text{g}/\text{mL}$ 388 treatment had little or no effect on the expression of MBP. In contrast, the level of MBP protein greatly decreased instead of increasing after the treatment of 100 $\mu\text{g}/\text{mL}$ 388 (Figure 5B). Additionally, experiment was carried out in spinal cord-derived cultures to determine the effect of 388 on the

expression of GFAP, a marker for astrocyte lineage. Exposure of the cells to 10 and 50 $\mu\text{g}/\text{mL}$ 388 resulted in a pronounced decrease in GFAP protein level. Interestingly, no significant change was observed at a higher concentration of 388 (100 $\mu\text{g}/\text{mL}$), when compared with that of control (Figure 5C).

388 Up-Regulates MeCP2 and Results in MeCP2-Mediated NSCs Differentiation

To elucidate the mechanism underlying the upregulation of neuron-related proteins by 388, we determined the change of

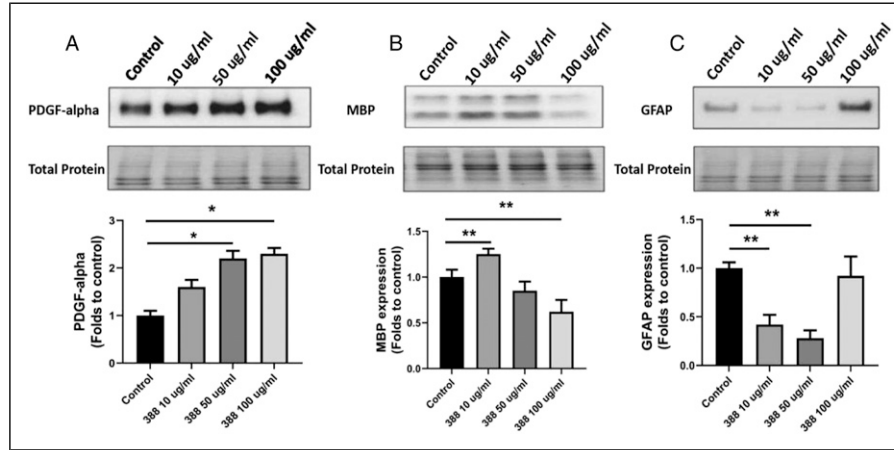


Figure 5. Differential effects of 388 on PDGF-alpha, MBP and GFAP expression. (A) PDGF-alpha expression from NSC treated with 10, 50 and 100 µg/mL 388 for 7 days of spontaneous differentiation. (B) MBP expression from NSC treated with 10, 50 and 100 µg/mL 388 for 7 days of spontaneous differentiation. (C) GFAP expression from NSC treated with 10, 50 and 100 µg/mL 388 for 7 days of spontaneous differentiation. Equal volumes of lysates with a total of 10 µg protein was applied to 12% TGX Stain-Free polyacrylamide gels. Total protein generated by stain-free visualization were used to ensure equivalent loading. One-way ANOVA followed by Bonferroni's Multiple Comparison Post-Test were performed to establish significant differences with control group: * $P < .05$; ** $P < .01$. The experiment was performed in triplicate. Results shown represent mean \pm SD from 3 independent experiments.

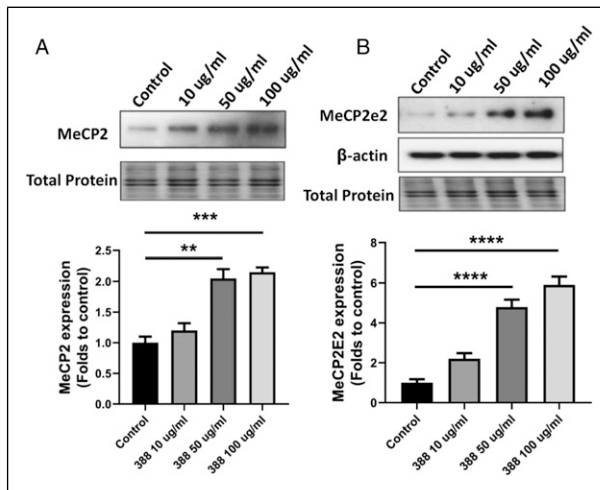


Figure 6. Treatment of 388 results in the upregulation of MeCP2 and its E2 isoform expressions. (A) MeCP2 expression from NSC treated with 10, 50, and 100 µg/mL 388 for 7 days of spontaneous differentiation. (B) MeCP2E2 expression from NSC treated with 10, 50, and 100 µg/mL 388 for 7 days of spontaneous differentiation. Equal volumes of lysates with a total of 10 µg protein was applied to 12% TGX Stain-Free polyacrylamide gels. Total protein generated by stain-free visualization were used to ensure equivalent loading. One-way ANOVA followed by Bonferroni's Multiple Comparison Post-Test were performed to establish significant differences with control group: ** $P < .05$; *** $P < .01$; **** $P < .001$. The experiment was performed in triplicate. Results shown represent mean \pm SD from 3 independent experiments. [Figure 8](#). Knockdown of MeCP2 by RNA interference blocks 388-mediated neurogenesis.

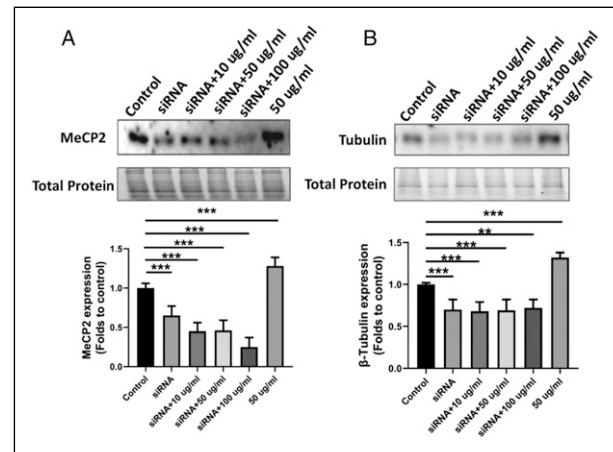


Figure 7. Knockdown of MeCP2 by RNA interference blocks 388-mediated neurogenesis. (A) MeCP2 expression from NSC treated with siRNA and 10, 50, and 100 µg/mL 388 for 7 days of spontaneous differentiation. (B) β-tubulin expression from NSC treated with siRNA and 10, 50, and 100 µg/mL 388 for 7 days of spontaneous differentiation. Equal volumes of lysates with a total of 10 µg protein was applied to 12% TGX Stain-Free polyacrylamide gels. Total protein generated by stain-free visualization were used to ensure equivalent loading. One-way ANOVA followed by Bonferroni's Multiple Comparison Post-Test were performed to establish. Significant differences with control group: ** $P < .01$; *** $P < .001$. The experiment was performed in triplicate. Results shown represent mean \pm SD from 3 independent experiments.

methyl CpG binding protein 2 (MeCP2) and one of its predominant E2 isoform of MeCP2 after treatment. In spinal cord-derived culture, a marked increase in MeCP2 and its

isoform level was observed after exposure to 388. These results suggest 388 has a stimulatory effect on MeCP2 expression ([Figure 6A and 6B](#)). To determine whether

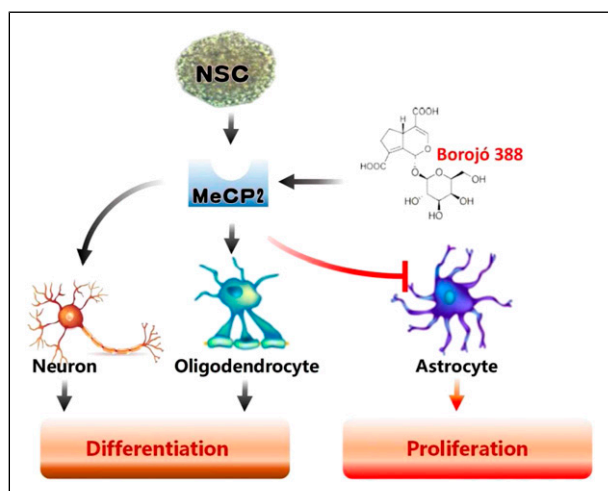


Figure 8. A proposed molecular mechanism of the active component 388 from Borojó, inhibits the proliferation of NSC and it is potent enough to direct neuronal and oligodendrocytic differentiation. Schematic representation the mechanism of action for 388 is via an effect on MeCP2 protein, a key molecule in cellular differentiation pathway. The astrocyte activity was inhibited when the dose of 388 was restricted under 100 $\mu\text{g}/\text{mL}$.

upregulation of neuron-related proteins by 388 occurs through MeCP2 pathway, cells were exposed to 388 at various concentrations in the presence of MeCP2 siRNA and the effect on β -tubulin protein, a marker for neuronal differentiation was investigated. Figure 7A proved that siRNA successfully knockdown the expression of MeCP2 and blocked the effect of 388 on MeCP2 levels. Consistently, pretreatment of MeCP2 siRNA abolished the stimulatory effect of 388 treatment on the expression of β -tubulin protein, supporting that MeCP2 mediates 388 induced neuronal differentiation. (Figure 7B).

Discussion

Results from this study show that the main active component 388 for Borojó promotes neuronal differentiation in nerve-derived stem cells and this is mediated by an effect on 388 on MeCP2 proteins. To our knowledge, this is the first study to demonstrate a neurotrophic effect of 388 on nerve stem cells. This discovery has important implications in developing iridoids as alternative and safe therapeutic agents from natural products and their applications in regenerative medicine. Neurodegenerative diseases including Alzheimer's disease, Parkinson's disease, Huntington's disease, multiple sclerosis, and amyotrophic lateral sclerosis are caused by neuronal loss and subsequent brain malfunction. Despite the development of drugs that can regulate NSC fate and facilitate the generation of neurons have been extensively pursued, their clinical application is far from being resolved. Natural Iridoid 388 has the advantage of regulating NSC fate and facilitating the generation of neurons or glial cells that aid the proper function of neurons. As it is a natural

fruit and can be safely consumed by humans. Thus, patients with neurodegeneration could intake natural Iridoids to increase neurogenesis from endogenous NSCs with minimal side effects. Moreover, understanding natural Iridoids' mechanism of action may help understand stem cell biology and speed up new drug development. For example, Iridoid glycoside Aucubin was found to have effect of facilitating neural precursor cell survival during neuronal differentiation. Aucubin preferably increased differentiated neurons that expressing GAD, a GABA synthesizing enzyme, suggesting that Iridoid glycoside may represent a potential therapeutic for Huntington's disease and epilepsy, which are characterized by the degeneration of GABAergic neurons.¹⁶ Cornel Iridoid glycoside protects against white matter lesions and demyelination by increasing myelin basic protein expression and the number of mature oligodendrocytes, and decreases the number of activated microglia and astrocytes via activation of the Brain-Derived Neurotrophic Factor (BDNF)/Neuregulin-1 Pathway.¹⁷

Collectively, these observations suggest that Iridoid glycosides have a broad range of biological effects, and the mechanisms may be related to promoting neuronal survival and providing a beneficial environment for brain repair. In order to identify additional novel naturally derived molecules that can regulate NSC fate, we screened several natural Iridoids and found that 388, isolated from Borojó, significantly promotes NSCs differentiation into neurons and oligodendrocyte lineage but overrides NSCs differentiation into astrocytes. Following mitogen withdrawal to initiate NSC differentiation, 388 treatment significantly up-regulates MeCP2 expression, providing one potential mechanism of action whereby 388 blocks proliferation and induces differentiation of NSCs through its action on MeCP2. The causal relationship is further demonstrated by an abolition of 388's effect on neuronal differentiation when MeCP2 was silenced. These results suggest that MeCP2 could be considered as a regulator of stem cell biology. As an essential epigenetic regulator in human brain development, in Rett patients, mutations in the X-linked MeCP2 gene causes the primary neurological disorder. Although many studies have devoted to specifying the role of MeCP2 and highlighting its contribution, the molecular mechanisms on stem cell biology in brain remain to be explored. MeCP2 protein binds to CPG dinucleotides, and the highest expression is detected in the brain, and specifically, it is highly expressed in neurons.¹⁸ MeCP2 expression upregulation occurs after differentiation and coincides with dendritic spine morphogenesis.¹⁹ Reduced expression of MeCP2 induces a decrease in proliferation and triggers the senescence and dysfunction of neural stem cells.¹¹ In the present study, we found that addition of 388 to the NSCs had highly significant effect on MeCP2 and its E2 isoform was specific, concurrent with increased neurogenesis evidenced by up-regulated MAP2, and TUJ1. Thus this effect is E2 isoform-specific.

In the presence of mitogen when NSCs proliferate and maintain their multipotency, the viability of NSCs treated with 388 was not affected when compared to that of control. In the absence of the growth factor, 388 increased neuronal differentiation, up to 1.8-folds of increase in MAP2 positive cell count, and resulting in significant reduction of proliferation at the dose of 10, 50, and 100 $\mu\text{g}/\text{mL}$ in spontaneous differentiation NSCs model. However, 388 showed differential effect on spinal cord-derived stem cells. Similar to brain-derived stem cells, neuron, oligodendrocyte precursors, and mature oligodendrocyte increased significantly, demonstrated by up-regulated pNFH, PDGFR- α , and MBP at the dose of 10 and 50 $\mu\text{g}/\text{mL}$ of 388. However, astrocytic marker GFAP decreases significantly. At the dose of 100 $\mu\text{g}/\text{mL}$, however, 388 induces an unexpected drop on neuronal and oligodendrocytic differentiation. A significantly higher expression of GFAP was also detected at the dose of 100 $\mu\text{g}/\text{mL}$. This suggests that 388 generally promotes neuronal differentiation but inhibits glial cell differentiation, exerting a cell-specific opposing effect. The dose-dependent trials can be used for determine effective and safe dose range for therapeutic applications. These results also indicate that spinal microglia may be also a target of 388, as spinal cord-derived culture contains 10% of microglia in total cell population,²⁰ and no microglia was detected in the cortex-derived culture model we used. This property may be utilized to promote neuronal cell differentiation while suppressing unwanted glial cell differentiation.

Interestingly MeCP2 knockdown also shows sign of astrogliosis in our study. This is in consistent with the study by Okabe Y. et al, and they reported that astrocytes from MeCP2 KO mice express higher levels of astrocyte related genes GFAP and S100b. MeCP2 is known to not only act as an activator but also as a repressor to downstream transcriptional changes. MeCP2 knockout decreases the excitatory amino acid transporter 1 and 2 (EAAT1/2) transcripts upon high glutamate exposure.²¹ Pacheco N.L. et al reported that in a MeCP2 deficient mice model, 46 out of 391 differentially expressed genes are astrocyte-specific, and the deficits in genes are associated with astrocyte maturation and morphology.²²

In conclusion, we show that the active component 388 from *Boroj*, inhibits the proliferation of NSC and it is potent enough to direct neuronal and oligodendrocytic differentiation. We have also identified the mechanism of action for 388 is via an effect on MeCP2 protein, a key molecule in cellular differentiation pathway. (Figure 8). However, to be further developed as a drug candidate that modulates NSCs, the dose should be restricted under 100 $\mu\text{g}/\text{mL}$ to prevent possible reactive astrocyte activation. However the detailed molecular mechanisms for 388 action on MeCP2 in neuronal differentiation remain to be explored. Nonetheless, an understanding of 388 action and its underlying mechanism may ultimately benefit patients suffering from neurodegenerative diseases.

Acknowledgments

The authors would like to thank all staff members in the Department of anesthesia, AnQing Municipal Hospitals of Anhui Medical University. The authors sincerely thank JiMing Kong and Tao Pan for their contributions to the whole trial design and his assistance with the study. The authors acknowledge BaoSheng Jing, Teng Guan, and DanGui Chen for their operation of this experiment, and authors acknowledge Prof HongJiao, who performed data extraction, and HaiMin Mai, who helped review the study design and data analysis. WeiBing Wang and Zhen Liu are responsible for the whole research conception, manuscript writing, and revision. All authors contributed toward data analysis, drafting, and critically revising the paper and agree to be accountable for all aspects of the work.

Declaration of Conflicting Interests

The author(s) declared no potential conflicts of interest with respect to the research, authorship, and/or publication of this article.

Funding

The author(s) received no financial support for the research, authorship, and/or publication of this article.

ORCID iDs

WeiBing Wang  <https://orcid.org/0000-0002-6059-7916>

BaoSheng Jing  <https://orcid.org/0000-0001-9833-3142>

References

1. Viljoen A, Mncwani N, Vermaak I. Anti-inflammatory iridoids of botanical origin. *Curr Med Chem*. 2012;19(14):2104-2127.
2. Lin L-C, Lee L-C, Huang C, et al. Effects of boschnalioside from *Boschniakia rossica* on dysglycemia and islet dysfunction in severely diabetic mice through modulating the action of glucagon-like peptide-1. *Phytomedicine*. 2019;62:152946.
3. Rathee D, Lather V, Singh Grewal A, Dureja H. Enzymatic inhibitory activity of iridoid glycosides from *Picrorrhiza kurroa* against matrix metalloproteinases: Correlating in vitro targeted screening and docking. *Comput Biol Chem*. 2019;78:28-36.
4. Zheng T, Peng J, Pei T, et al. Cornel iridoid glycoside exerts a neuroprotective effect on neuroinflammation in rats with brain injury by inhibiting NF- κ B and STAT3. *3 Biotech*. 2019;9(5): 195.
5. Ma D, Wang N, Fan X, et al. Protective effects of cornel iridoid glycoside in rats after traumatic brain injury. *Neurochem Res*. 2018;43(4):959-971.
6. Min KimSim YU-C, Shin Y, Kwon YK. Aucubin promotes neurite outgrowth in neural stem cells and axonal regeneration in sciatic nerves. *Exp Neurobiol*. 2014;23(3):238-245.
7. Yao R-Q, Zhang L, Wang W, Li L. Cornel iridoid glycoside promotes neurogenesis and angiogenesis and improves neurological function after focal cerebral ischemia in rats. *Brain Res Bull*. 2009;79(1):69-76.
8. Rabelo Rodrigues F, de Souza Ramos A, Fernandes Amaral AC, Pinto Ferreira JL, da Silva Carneiro C, Rocha de Andrade Silva

- J. Evaluation of Amazon fruits: Chemical and nutritional studies on *Borojoa sorbilis*. *J Sci Food Agric*. 2018;98(10):3943-3952.
9. Alessio N, Riccitiello F, Squillaro T, et al. Neural stem cells from a mouse model of Rett syndrome are prone to senescence, show reduced capacity to cope with genotoxic stress, and are impaired in the differentiation process. *Exp Mol Med*. 2018;50(1):1.
 10. Ma T-T, Li X-F, Li W-X, et al. Geniposide alleviates inflammation by suppressing MeCP2 in mice with carbon tetrachloride-induced acute liver injury and LPS-treated THP-1 cells. *Int Immunopharmacol*. 2015;29(2):739-747.
 11. Chaves-López C, Usai D, Gavino Donadu M, et al. Potential of *Borojoa patinoi* Cuatrecasas water extract to inhibit nosocomial antibiotic resistant bacteria and cancer cell proliferation in vitro. *Food Funct*. 2018;9(5):2725-2734.
 12. Ohashi M, Korsakova E, Allen D, et al. Loss of MECP2 leads to activation of P53 and neuronal senescence. *Stem Cell Rep*. 2018;10(5):1453-1463.
 13. Liang G, Liang Z, Jiao H, Pan T, Lu W, Huang J. Extraction and preparation methods of Borojo active constituent and its antibacterial activity and antioxidant property, 2013, Patent number: ZL201110236556.7; Authorisation number: CN 102351927 B; Date of authorisation: 2013.12.18.
 14. Lu Y, Xu F, Li J, Jiao H, Liu B. In vitro antioxidant activity of *Borojoa sorbilis* Custer. *J Int Pharm Res*. 2013;40:718.
 15. Jing Z, Hong J, Wang JJ, Chen XY, Meng P. Anti-aging effects of concentrated powder of Borojo fruit on aging mice induced by D-Galactose. *Food Sci*. 2013;34:293.
 16. Song M, Han M, Kim Kwon Y. Effect of aucubin on neural precursor cell survival during neuronal differentiation. *Int J Neurosci*. 2018;128(10):899-905.
 17. Wang M, Hua X, Niu H, et al. Cornel iridoid glycoside protects against white matter lesions induced by cerebral ischemia in rats via activation of the brain-derived neurotrophic factor/neuregulin-1 pathway. *Neuropsychiatr Dis Treat*. 2019;15:3327-3340.
 18. Luikenhuis S, Giacometti E, Beard CF, Jaenisch R. Expression of MeCP2 in postmitotic neurons rescues Rett syndrome in mice. *Proc Natl Acad Sci U S A*. 2004;101(16):6033-6038.
 19. Gulmez Karaca K, Brito DVC, Oliveira AMM. MeCP2: A critical regulator of chromatin in neurodevelopment and adult brain function. *Int J Mol Sci*. 2019;20(18):4577.
 20. Pang Y, Zheng B, Kimberly SL, Cai Z, Rhodes PG, Lin RCS. Neuron-oligodendrocyte myelination co-culture derived from embryonic rat spinal cord and cerebral cortex. *Brain Behav*. 2012;2(1):53-67.
 21. Okabe Y, Takahashi T, Mitsumasa C, Kosai K-I, Tanaka E, Matsuiishi T. Alterations of gene expression and glutamate clearance in astrocytes derived from an MeCP2-null mouse model of Rett syndrome. *PLoS One*. 2012;7(4):e35354.
 22. Pacheco NL, Heaven MR, Holt LM, et al. RNA sequencing and proteomics approaches reveal novel deficits in the cortex of MeCP2-deficient mice, a model for Rett syndrome. *Mol Autism*. 2017;8:56.